

Geology

Sea-level-induced seismicity and submarine landslide occurrence

Daniel S. Brothers, Karen M. Luttrell and Jason D. Chaytor

Geology published online 22 July 2013;
doi: 10.1130/G34410.1

Email alerting services click www.gsapubs.org/cgi/alerts to receive free e-mail alerts when new articles cite this article

Subscribe click www.gsapubs.org/subscriptions/ to subscribe to *Geology*

Permission request click <http://www.geosociety.org/pubs/copyrt.htm#gsa> to contact GSA

Copyright not claimed on content prepared wholly by U.S. government employees within scope of their employment. Individual scientists are hereby granted permission, without fees or further requests to GSA, to use a single figure, a single table, and/or a brief paragraph of text in subsequent works and to make unlimited copies of items in GSA's journals for noncommercial use in classrooms to further education and science. This file may not be posted to any Web site, but authors may post the abstracts only of their articles on their own or their organization's Web site providing the posting includes a reference to the article's full citation. GSA provides this and other forums for the presentation of diverse opinions and positions by scientists worldwide, regardless of their race, citizenship, gender, religion, or political viewpoint. Opinions presented in this publication do not reflect official positions of the Society.

Notes

Advance online articles have been peer reviewed and accepted for publication but have not yet appeared in the paper journal (edited, typeset versions may be posted when available prior to final publication). Advance online articles are citable and establish publication priority; they are indexed by GeoRef from initial publication. Citations to Advance online articles must include the digital object identifier (DOIs) and date of initial publication.

Sea-level-induced seismicity and submarine landslide occurrence

Daniel S. Brothers¹, Karen M. Luttrell², and Jason D. Chaytor¹

¹U.S. Geological Survey, Coastal and Marine Science Center, 384 Woods Hole Road, Woods Hole, Massachusetts 02543, USA

²U.S. Geological Survey, Volcano Science Center, 345 Middlefield Road, MS 910, Menlo Park, California 94025, USA

ABSTRACT

The temporal coincidence between rapid late Pleistocene sea-level rise and large-scale slope failures is widely documented. Nevertheless, the physical mechanisms that link these phenomena are poorly understood, particularly along nonglaciated margins. Here we investigate the causal relationships between rapid sea-level rise, flexural stress loading, and increased seismicity rates along passive margins. We find that Coulomb failure stress across fault systems of passive continental margins may have increased more than 1 MPa during rapid late Pleistocene–early Holocene sea-level rise, an amount sufficient to trigger fault reactivation and rupture. These results suggest that sea-level–modulated seismicity may have contributed to a number of poorly understood but widely observed phenomena, including (1) increased frequency of large-scale submarine landslides during rapid, late Pleistocene sea-level rise; (2) emplacement of coarse-grained mass transport deposits on deep-sea fans during the early stages of marine transgression; and (3) the unroofing and release of methane gas sequestered in continental slope sediments.

INTRODUCTION

Submarine slope failures, or landslides, occur on every continental margin and play a central role in our understanding of margin evolution, deep-water depositional processes, and coastal tsunamigenic hazards. The resulting mass transport deposits represent an enormous volume of sediment that has been redistributed from shallow-water depocenters to deep-sea fan systems. One of the major challenges in global geohazards research is to unravel the cause and effect relationships between submarine landslides and climate change.

Previous studies observed causal relationships between water loading and fault rupture (Brothers et al., 2011), as well as sea-level rise and magmatic activity (Kutterolf et al., 2013). Although earthquakes are the most commonly invoked triggering mechanism for slope failures along glaciated continental margins, few studies have examined the links between seismicity rates and global hydroclimatic variations along nonglaciated passive margins. Because large earthquakes are relatively uncommon along passive margins, transient variations in seismicity rates may be expected to leave behind noticeable or even catastrophic signatures in the geologic record.

This paper tests the effects of flexural stress loading of passive margins during rapid sea-level transgression (Luttrell and Sandwell, 2010). We propose that water mass redistribution and temporarily elevated seismicity may contribute to the following phenomena observed in the late Pleistocene–early Holocene geologic record: (1) an apparent increase in submarine landslide frequency (Lee, 2009; Leynaud et al., 2009; Maslin et al., 2004; Owen et al., 2007); (2) unexpected deep-water sandy turbidite and debris flow deposition during sea-level transgression (Kolla and Perlmutter, 1993); and (3) punctuated increases in atmospheric methane concentration due to release of sequestered methane hydrates along continental margins (Maslin et al., 2010).

TIMING AND IMPLICATIONS OF SUBMARINE SLOPE FAILURES

For a slope to fail it first needs to be preconditioned for failure; then it typically requires an external perturbation, or trigger, to induce sudden increases in substrate pore pressure and reduced shear strength of sedimentary deposits. Changes in the slope deposition rate, sediment texture,

hydrate stability, fluid discharge, salt diapirism, and slope gradient are factors that can precondition slopes for failure, and each of these factors can be influenced by hydroclimatic changes. Assigning a triggering mechanism to failures observed in the geologic record is difficult, particularly along passive margins where earthquakes are infrequent and paleoseismic records are poorly developed.

Coincident timing between sea-level variation and the emplacement of deep-water mass transport deposits is widely documented along passive margins (see Table DR1 in the GSA Data Repository¹). In this paper we compile age data for two categories of slope failures and their associated deposits: (1) discrete, large-scale failures, or landslides, that have an identifiable source region and geomorphic expression, and (2) coarse-grained deep-sea fan and/or apron deposits that have not been matched with individual failures, but were likely sourced from numerous failures along a relatively broad section of the slope. Age distributions of both categories are perplexing: the frequency of large-scale slope failures appears to be highest during late Pleistocene–early Holocene eustatic sea-level rise (e.g., Maslin et al., 2004; Lee, 2009); coarse-grained mass transport deposition in several deep-sea fan systems continued well into the later stages of marine transgression, contrary to expectations from widely accepted sequence stratigraphic models (Kolla and Perlmutter, 1993).

During relative sea-level lowstands, sediment delivery to continental shelf edge and slope is expected to increase along both glacial and nonglacial passive margins, providing a source of potentially unstable sedimentary deposits. Postglacial isostatic rebound and elevated seismicity during the past 15 k.y. provides one plausible triggering mechanism for slope failures along high-latitude margins (Bungum et al., 2005; Klemann and Wolf, 1998; Wu and Johnston, 2000), but causes for temporally clustered slope failures along nonglaciated passive margins are poorly understood (Maslin et al., 2004; Owen et al., 2007).

The removal of several hundred meters of overburden during large-scale slope failures has the potential to release vast quantities of methane stored in marine sediments. Kennett et al. (2003) suggested that destabilization of sequestered gas hydrates is the primary control on atmospheric methane variation during the Quaternary. However, the links between hydrate dissociation, submarine landslides, and global climate change remain controversial (Maslin et al., 2010; Sowers, 2006), and hydrate dissociation as a triggering mechanism is difficult to establish without evidence for coeval increases in bottom-water temperature, particularly for the many landslides located at water depths >1500 m (Twichell et al., 2009).

DATA AND METHODS

In general, Atlantic-type passive margins contain fault systems that developed during continental rifting and later became inactive during post-rift margin evolution. The accumulation of thick, post-rift sedimentary prisms that underlie the shelf, slope, and rise leads to gravitationally induced stresses and thin-skinned tectonics (Rowan et al., 2004), including normal, reverse, and low-angle faults confined to the upper few kilometers of sediment. Although the paleoseismic history along passive margins is usually poorly known, any of the fault systems have the potential to be reactivated by external stress perturbations.

¹GSA Data Repository item 2013274, table of landslide age estimates, description of stress modeling parameters, structural cross sections, and model sensitivity tests, is available online at www.geosociety.org/pubs/ft2013.htm, or on request from editing@geosociety.org or Documents Secretary, GSA, P.O. Box 9140, Boulder, CO 80301, USA.

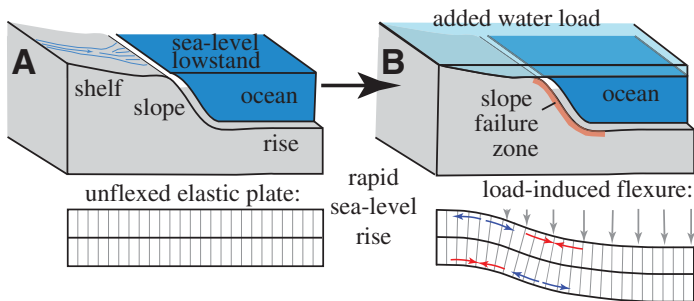


Figure 1. Conceptual models for flexural loading of continental margin following rapid eustatic sea-level rise. A: Margin configuration prior to sea-level rise. B: Configuration following rapid sea-level rise. Added load of water on shelf induces flexural bending stresses on underlying elastic plate (red arrows are compression; blue arrows are tension).

During and immediately after eustatic sea-level rise, a given margin will respond to the weight of the new water load through lithospheric flexure (Fig. 1). The amount that fault systems in coastal regions are affected by ocean loading stresses primarily depends on the thickness of the flexing plate, the geometry of the ocean basin (i.e., bathymetry), and the orientation of faults relative to the coastline. We combined global bathymetric data with a late Pleistocene eustatic sea-level curve (Peltier and Fairbanks, 2006) to generate an accurate loading history for nonglacial margins of the Atlantic, Gulf of Mexico, and Mediterranean basins.

The magnitude of bending-induced fault stress is estimated by isolating the effects of sea-level-induced flexure. The full three-dimensional stress tensor due to rapid sea-level rise was calculated within an elastic plate that overlies a Maxwell viscoelastic half-space (Luttrell and Sandwell, 2010; see the Data Repository). For both the plate and the half-space, we calculate the fully relaxed stress state and use an elastic plate thickness of $H = 50$ km for global calculations, then calculate regional perturbations using elastic thickness constraints from previous studies. Figure 2A shows the modeled maximum shear stress perturbations [$(\sigma_1 - \sigma_3)/2$] expected from sea-level-induced bending; other sources of crustal stress acting over longer time scales, such as tectonic driving forces, are not included in this calculation.

We selected the Amazon and North Carolina margins (Figs. 2B and 2C) as representative end members for wide (>200 km shelf width) and narrow (<100 km shelf width) passive margins. These margins were selected because (1) the lithospheric structure is relatively well known (Klitgord et al., 1988; Watts et al., 2009; Wyer and Watts, 2006); (2) they contain structural features common to rifted passive margins, including basement normal faults that formed during continental rifting and relatively shallow, thin-skinned normal and reverse faults beneath the outer shelf and slope (Fig. DR1 in the Data Repository); and (3) large slope failures were triggered on both margins during late Pleistocene sea-level transgression (Figs. 2B and 2C). Models used $H = 35$ and $H = 20$ km for the Amazon and North Carolina margins, respectively (Watts et al., 2009; Wyer and Watts, 2006). The three-dimensional stress tensor was resolved into Coulomb failure stresses (ΔC_f ; Fig. 3), allowing us to identify areas where fault rupture would have been promoted ($\Delta C_f > 0$) or inhibited ($\Delta C_f < 0$) during and after 120 m of sea-level rise. ΔC_f was estimated across hypothetical faults embedded in the following structural domains (Fig. 3): basement normal faults of the continental hinge zone and oceanic crust, thin-skinned normal faults near the shelf edge, and thin-skinned reverse faults below the shelf edge and slope. The coefficients of friction for basement and thin-skinned faults in the models are set to $\mu = 0.6$ and $\mu = 0.1$, respectively.

RESULTS

Following 120 m of sea-level rise, models predict increased maximum shear stress at seismogenic depths (~ 10 km). Where these bending stresses inhibit or promote fault rupture depends on the elastic thickness and geometry of affected faults. Cross-sectional models of nonglacial margins (Fig. 3; Figs. DR2 and DR3) suggest that rupture is promoted across at least one fault domain located within 100 km of the continental slope, regardless of margin geometry and elastic thickness (e.g., $H = 15, 20, 35$, and 50 km). For example, rupture is promoted along the Amazon margin (Fig. 3A) for both the hinge-zone basement faults and the thin-skinned normal faults near the shoreline ($\Delta C_f > 1$ MPa); rupture is strongly inhibited ($\Delta C_f < 0$) across the deep crystalline and thin-skinned normal faults below the outer shelf and upper slope; and rupture is promoted ($0.1 < \Delta C_f < 0.3$ MPa) on the reverse faults beneath the continental slope. Similar patterns are observed along the United States Mid-Atlantic margin, but the narrower continental shelf and lower elastic thickness promotes rupture of

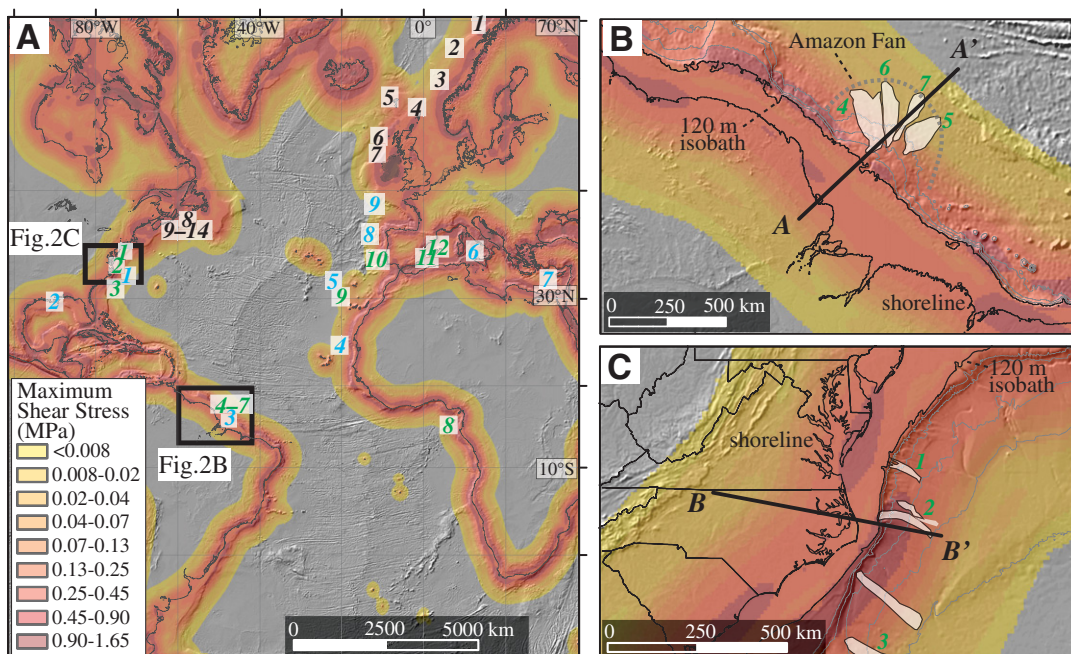


Figure 2. A: Maximum shear stress perturbation from ocean loading on 50-km-thick plate (10 km calculation depth). Numbered locations represent dated submarine mass transport deposits (Table DR1; see footnote 1) separated into nonglacial margins (green), nonglacial deep-sea fan deposits (blue), and glacial margins (black). Dashed boxes are enlarged views. B: Amazon margin. C: North Carolina margin. A-A' and B-B' are cross sections shown in Figure 3; shaded regions outline individual landslides (Maslin et al., 1998; Twichell et al., 2009).

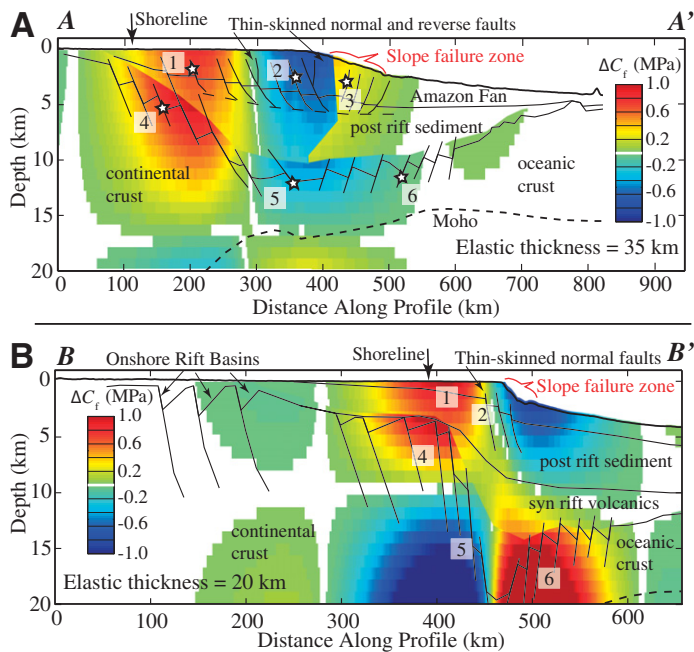


Figure 3. Coulomb failure stress models (ΔC_f) resulting from 120 m of eustatic sea-level rise. A: Along Amazon margin. Numbered stars are ΔC_f calculations for individual faults shown in Figure 4A. B: Along North Carolina margin. Fault rupture is promoted where $\Delta C_f > 0$ and inhibited where $\Delta C_f < 0$. Calculations are performed over several tectonic domains: 1—coastal normal faults, 2—shelf-edge normal faults, 3—slope reverse faults, 4—continental hinge-zone normal faults, 5—transitional normal faults, 6—oceanic normal faults.

basement faults within 80 km of the continental slope (Fig. 3B). In general, the time interval having the most rapid increase in sea level (ca. 16–9 ka) coincides with the greatest variation in ΔC_f (Fig. 4A), the greatest concentration of submarine landslides along glacial and nonglacial margins (Fig. 4B), as well as the approximate cessation of coarse-grained deposition on several deep-sea fan systems (Table DR1).

DISCUSSION

Since 125 ka, ~50% of the total volume of submarine sediment mobilized during extreme slope failures occurred between 15 and 8 ka (Korup, 2012). The clustering of deposits dated to ca. 15 ka and ca. 11 ka (blue dots in Fig. 4B) may be associated with major meltwater pulses 1A and 1B (Maslin et al., 2004). During the most recent sea-level lowstand (50–18 ka), depositional processes of the outer shelf and upper slope were relatively uniform, and in many places terrigenous sediment fluxes were low compared to the subsequent interval from 19 to 8 ka. If we assume that lithospheric stresses were not modulated by transient environmental perturbations, faults may have steadily accumulated background stress for thousands of years without rupture. The coincident timing of failure events may suggest that continental slopes were preconditioned for failure and had a common triggering mechanism.

During and immediately after the Last Glacial Maximum (LGM), global eustatic sea level was nearly 120 m lower than at present, which allowed for extensive accumulation of potentially unstable shelf-edge and slope deposits (Lee, 2009). During the transition from glacial to interglacial time (ca. 16–8 ka), continental ice sheets were receding and eustatic sea level was rising 10–20 mm/yr. Although the concentration of submarine landslides along both high- and low-latitude margins during this time period is distinct (Fig. 4B), our results are most pertinent to margins unaffected by glacial isostatic adjustment. We propose that the added load of water on the continental shelves generated flexural stresses capable of

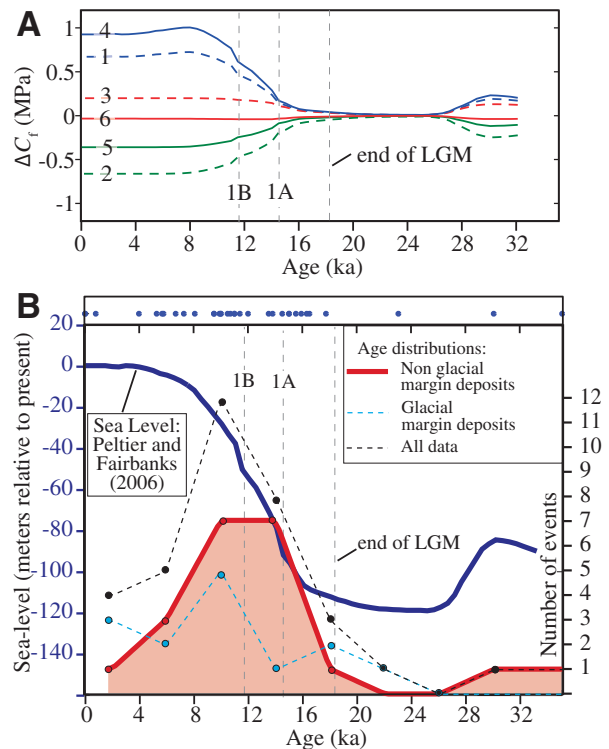


Figure 4. A: Coulomb failure stress, ΔC_f , time series for receiver faults in Figure 3A. Dashed vertical lines are end of Last Glacial Maximum (LGM) and meltwater pulses 1A and 1B (Kennett et al., 2003). B: Age distributions for submarine mass transport deposits (blue dots are mid-point of age range; Table DR1; see footnote 1). All distributions are based on 4 k.y. bin widths.

promoting rupture along critically stressed fault systems, which in turn may have triggered widespread slope failure.

On both wide and narrow margins, deep basement faults near the modern-day shoreline are potential sources of large, infrequent earthquakes; $M > 7$ earthquakes may induce a catastrophic slope failure more than 100 km from the hypocenter (ten Brink et al., 2009). During rapid sea-level rise, these faults undergo an increase in ΔC_f of >1.2 MPa, an order of magnitude greater than the accepted threshold of 0.1 MPa needed to promote fault rupture (King et al., 1994). Although thin-skinned faults beneath the continental slope are likely weak and incapable of generating large earthquakes, rupture may increase the pore fluid pressure and/or local seabed gradient, thus triggering slope failures. The maximum ΔC_f for wide margins is >100 km from the shelf edge, suggesting that slope failure may be linked to rupture of thin-skinned faults (Fig. 3A). Narrow margins (e.g., U.S. Mid-Atlantic, western Africa, Iberia, and central South America) are more likely to undergo maximum ΔC_f across seismogenic basement faults located within 100 km of the shelf edge (e.g., Fig. 3B).

Despite very limited paleoseismic data and the relative infrequency of large earthquakes along passive margins, seismicity is the most commonly invoked triggering mechanism for slope failures (e.g., Owen et al., 2007). For example, modern-day seismicity rates along the U.S. Atlantic margin suggest that an $M \geq 7.0$ earthquake occurs somewhere along the margin every few thousand years (ten Brink et al., 2009). Strong motion and stress drops associated with earthquakes on faults with such large recurrence intervals may be higher than faults having shorter recurrence intervals (Kanamori and Allen, 1986). Along high-latitude margins proximal to glacial ice masses, sea-level-induced crustal stresses are expected to be less significant than those generated by glacial isostatic adjustment (Bungum et al., 2005; Klemann and Wolf, 1998; Wu and Johnston, 2000).

However, the way that ocean loading and glacial unloading stresses interact along specific margins may be complicated and requires further study.

The potential relationship between submarine landslides and climate change may have far-reaching implications. First, widespread slope failure appears to have a temporal correlation with punctuated increases in atmospheric methane concentration and major meltwater pulses between 15–13 and 11–8 ka. Though speculative, sea-level–induced seismicity and subsequent failure of unstable slopes may have unroofed methane hydrate deposits, leading to destabilization and release of methane gas into the oceans and atmosphere (Maslin et al., 2004, 2010; Sowers, 2006; Fig. 4B). Second, coarse-grained deep-sea fan deposits emplaced during the middle and late stages of marine transgression (ca. 15–9 ka) posed problems to the original sequence stratigraphic models; previous studies focused on linking these deposits with increased fluvial runoff and sediment supply during marine transgression (Kolla and Perlmutter, 1993). Without direct evidence for fluvial transport and bypass of the outer shelf and/or upper slope (e.g., hyperpycnal flows), earthquake-induced postdepositional failure and remobilization of shelf-edge–upper slope sediment may provide an alternative source for these coarse-grained, deep-sea fan deposits.

CONCLUSIONS

We conclude that eustatic sea-level rise has the potential to induce bending stresses that can lead to elevated seismicity. Our results suggest that rapid sea-level rise between ca. 15 and 8 ka promoted rupture of passive margin fault systems, which in turn may have triggered landslides on the adjacent continental slopes and upper rises. Such a cause and effect relationship may help us understand feedbacks between slope stability and climate change by providing a mechanism for sudden destabilization and release of seabed methane into the ocean and atmosphere.

ACKNOWLEDGMENTS

We thank Uri ten Brink, Brian Andrews, Donna Shillington, and Matt Owen for their helpful reviews. The U.S. Geological Survey Mendenhall Postdoc Program and the U.S. Nuclear Regulatory Commission provided support for this research. The U.S. Government does not make any warranty, express or implied, nor assume any legal liability or responsibility for the accuracy, completeness, or usefulness of any information, apparatus, product, or process disclosed, nor represent that its use would not infringe on privately owned rights.

REFERENCES CITED

- Brothers, D., Kilb, D., Luttrell, K., Driscoll, N., and Kent, G., 2011, Loading of the San Andreas fault by flood-induced rupture of faults beneath the Salton Sea: *Nature Geoscience*, v. 4, p. 486–492, doi:10.1038/ngeo1184.
- Bungum, H., Lindholm, C., and Faleide, J.I., 2005, Postglacial seismicity offshore mid-Norway with emphasis on spatio-temporal-magnitudinal variations: *Marine and Petroleum Geology*, v. 22, p. 137–148, doi:10.1016/j.marpetgeo.2004.10.007.
- Kanamori, H., and Allen, C.R., 1986, Earthquake repeat time and average stress drop, *in* Das, S., et al., eds., *Earthquake source mechanics*: American Geophysical Union Geophysical Monograph 37, p. 227–235, doi:10.1029/GM037p0227.
- Kennett, J.P., Cannariato, K.G., Hندی, I.L., and Behl, R.J., 2003, Methane hydrates in Quaternary climate change: The clathrate gun hypothesis: Washington, D.C., American Geophysical Union, 213 p., doi:10.1029/054SP.
- King, G.C.P., Stein, R.S., and Lin, J., 1994, Static stress changes and the triggering of earthquakes: *Seismological Society of America Bulletin*, v. 84, p. 935–953.
- Klemann, V., and Wolf, D., 1998, Modelling of stresses in the Fennoscandian lithosphere induced by Pleistocene glaciations: *Tectonophysics*, v. 294, p. 291–303, doi:10.1016/S0040-1951(98)00107-3.
- Klitgord, K.D., Hutchinson, D.R., and Schouten, H., 1988, U.S. Atlantic continental margin; structural and tectonic framework, *in* Sheridan, R.E., and Grow, J.A., eds., *The Atlantic Continental Margin: U.S.*: Boulder, Colorado, Geological Society of America, *Geology of North America*, v. I-2, p. 19–55.
- Kolla, V., and Perlmutter, M.A., 1993, Timing of turbidite sedimentation on the Mississippi Fan: *American Association of Petroleum Geologists Bulletin*, v. 77, p. 1129–1141.
- Korup, O., 2012, Earth's portfolio of extreme sediment transport events: *Earth-Science Reviews*, v. 112, p. 115–125, doi:10.1016/j.earscirev.2012.02.006.
- Kutterolf, S., Jegen, M., Mitrovica, J.X., Kwasnitschka, T., Freundt, A., and Huybers, P.J., 2013, A detection of Milankovitch frequencies in global volcanic activity: *Geology*, v. 41, p. 227–230, doi:10.1130/G33419.1.
- Lee, H.J., 2009, Timing of occurrence of large submarine landslides on the Atlantic Ocean margin: *Marine Geology*, v. 264, p. 53–64, doi:10.1016/j.margeo.2008.09.009.
- Leynaud, D., Mienert, J., and Vanneste, M., 2009, Submarine mass movements on glaciated and non-glaciated European continental margins: A review of triggering mechanisms and preconditions to failure: *Marine and Petroleum Geology*, v. 26, p. 618–632, doi:10.1016/j.marpetgeo.2008.02.008.
- Luttrell, K., and Sandwell, D., 2010, Ocean loading effects on stress at near shore plate boundary fault systems: *Journal of Geophysical Research*, v. 115, B08411, doi:10.1029/2009JB006541.
- Maslin, M., Mikkelsen, N., Vilela, C., and Haq, B., 1998, Sea-level– and gas-hydrate–controlled catastrophic sediment failures of the Amazon Fan: *Geology*, v. 26, p. 1107–1110, doi:10.1130/0091-7613(1998)026<1107:SLAGHC>2.3.CO;2.
- Maslin, M., Owen, M., Day, S., and Long, D., 2004, Linking continental-slope failures and climate change: Testing the clathrate gun hypothesis: *Geology*, v. 32, p. 53–56, doi:10.1130/G20114.1.
- Maslin, M., Owen, M., Betts, R., Day, S., Dunkley Jones, T., and Ridgwell, A., 2010, Gas hydrates: Past and future geohazard?: *Royal Society of London Philosophical Transactions*, v. 368, p. 2369–2393, doi:10.1098/rsta.2010.0065.
- Owen, M., Day, S., and Maslin, M., 2007, Late Pleistocene submarine mass movements: Occurrence and causes: *Quaternary Science Reviews*, v. 26, p. 958–978, doi:10.1016/j.quascirev.2006.12.011.
- Peltier, W.R., and Fairbanks, R.G., 2006, Global glacial ice volume and Last Glacial Maximum duration from an extended Barbados sea level record: *Quaternary Science Reviews*, v. 25, p. 3322–3337, doi:10.1016/j.quascirev.2006.04.010.
- Rowan, M.G., Peel, F.J., and Vendeville, B.C., 2004, Gravity-driven fold belts on passive margins, *in* McClay, K.R., ed., *Thrust tectonics and hydrocarbon systems*: American Association of Petroleum Geologists Memoir 82, p. 157–182.
- Sowers, T., 2006, Late Quaternary atmospheric CH₄ isotope record suggests marine clathrates are stable: *Science*, v. 311, p. 838–840, doi:10.1126/science.1121235.
- ten Brink, U.S., Lee, H.J., Geist, E.L., and Twichell, D., 2009, Assessment of tsunami hazard to the US East Coast using relationships between submarine landslides and earthquakes: *Marine Geology*, v. 264, p. 65–73, doi:10.1016/j.margeo.2008.05.011.
- Twichell, D.C., Chaytor, J.D., ten Brink, U.S., and Buczkowski, B., 2009, Morphology of late Quaternary submarine landslides along the US Atlantic continental margin: *Marine Geology*, v. 264, p. 4–15, doi:10.1016/j.margeo.2009.01.009.
- Watts, A.B., Rodger, M., Peirce, C., Greenroyd, C.J., and Hobbs, R.W., 2009, Seismic structure, gravity anomalies, and flexure of the Amazon continental margin, NE Brazil: *Journal of Geophysical Research*, v. 114, B07103, doi:10.1029/2008JB006259.
- Wu, P., and Johnston, P., 2000, Can deglaciation trigger earthquakes in N. America?: *Geophysical Research Letters*, v. 27, p. 1323–1326, doi:10.1029/1999GL011070.
- Wyer, P., and Watts, A.B., 2006, Gravity anomalies and segmentation at the East Coast, USA continental margin: *Geophysical Journal International*, v. 166, p. 1015–1038, doi:10.1111/j.1365-246X.2006.03066.x.

Manuscript received 23 January 2013

Revised manuscript received 22 April 2013

Manuscript accepted 27 April 2013

Printed in USA